Molecular Energy and Electron Transfer Assemblies Made of Self-Organized Lipid-Porphyrin Bilayer Vesicles

Teruyuki Komatsu, Miho Moritake, and Eishun Tsuchida*[a]

Abstract: Novel molecular energy and electron transfer assemblies in vesicular form, which are made of self-organized amphiphilic porphyrins bearing phospholipid-like substituents (lipid-porphyrins), have been photochemically characterized. Tetraphenylporphyrin (TPP) derivatives with four dialkylphosphocholine groups [free-base (**1a**), Zn^{2+} complex (**1b**), and Fe^{3+} complex (**1c**)] are spontaneously associated in water to form spherical unilamellar vesicles with a diameter of 100–150 nm. Exciton calculations based on the bilayered sheet model of **1b**, which has a porphyrin packing similar to that seen in the triclinic unit cell of the Zn^{2+}TPP crystals, reproduced the Soret band bathochromic shift appearing in the aqueous solution of **1b** well. The UV/Vis absorption spectrum of the **1a**/**1b** hybrid vesicles (molar ratio: 1/1) showed no electronic interaction between the two porphyrin chromophores in the ground state, but efficient intermolecular singlet–singlet energy transfer took place from the excited **1b** donors to the **1a** acceptor within the vesicle. Near-field scanning optical microspectroscopy of the **1a**/**1b** vesicles on a graphite surface also showed only free-base porphyrin fluorescence. The efficiency of the energy transfer was 0.81 and the rate constant was $3.1 \times 10^9\ s^{-1}$. On the other hand, protoporphyrin IX bearing two alkylphosphocholine propionates (**2**) was incorporated into the **1a** or **1c** bilayer vesicles (ca. 100 nm ϕ, molar ratio: **1a**/**2** or **1c**/**2** = 10). The UV/Vis absorption spectrum showed that **2** was successfully anchored into the fluid alkylene region of the membrane without stacking. Photoirradiation (λ_{ex}: 390 nm) of the **1c**/**2** vesicles in the presence of triethanolamine led a vectorial electron transfer from the outer aqueous phase to the membrane center, which allowed reduction of the ferric ion of the Fe^{3+}TPP platform.

Keywords: electron transfer · energy transfer · porphyrinoids · self-assembly · vesicles

Introduction

In nature, solar energy conversion is triggered by the capturing of sunlight by hundreds of chlorophyll arrays. That excited energy is funneled to a reaction center by an extremely efficient transfer of energy and is converted to chemical potential in the form of a long-lived charge-separated state.[1] To obtain insight into these natural light-harvesting events, numerous porphyrinoid arrays linked by covalent bonds have been synthesized.[2, 3] Nonetheless, general organic synthetic procedures did not allow the construction of a large-scale supramolecular architecture in which more than hundreds of metalloporphyrins are ordered with great regularity. Thus, noncovalent approaches could present considerable advantages.[4, 5] Furthermore, if we are to reproduce any biochemical reaction, the aqueous medium is particularly important. From these points of view, self-organized porphyrin assemblies have attracted attention as a potential light-harvesting antennae model in water. Whereas porphyrin H-aggregates are generally quenched due to the large exciton couplings,[6] J-aggregated porphyrins show strong fluorescence.[7] One of the most significant examples of the emitting assemblies is our spherical bilayered vesicles made of amphiphilic tetraphenylporphyrin (TPP) with four phospholipid-like substituents (lipid-porphyrin, **1a**); its fluo-

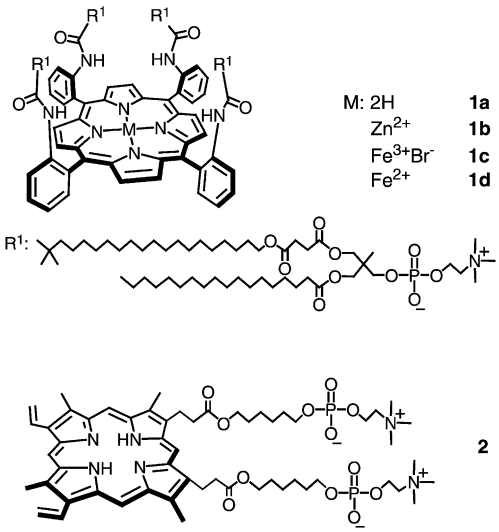

[a] Prof. E. Tsuchida, Dr. T. Komatsu, M. Moritake
Advanced Research Institute for Science and Engineering Waseda University, Tokyo 169-8555 (Japan)
Fax: (+81) 3-3205-4740
E-mail: eishun@waseda.jp

DOI: 10.1002/chem.200305013

rescence intensity remained 76% of that of the monomer in organic solvent.[8] Herein, we report on novel bilayer vesicles consisting of two lipid-porphyrin ensembles [free-base (**1a**) and Zn^{2+} complex (**1b**)], in which an efficient singlet–singlet energy transfer took place based on the in-plane tightest packing of the porphyrin platforms. In addition, we present vectorial electron migration from the bulk aqueous phase to the membrane center of the Fe^{3+} complex lipid–porphyrin (**1c**) vesicles. The amphiphilic protoporphyrin IX (**2**) anchored into the highly oriented alkylchain region acts as an electron transfer mediator. Photoirradiation (λ_{ex}: 390 nm) under the coexistence of triethanolamine allowed reduction of the central ferric ions of the Fe^{3+} porphyrins and gave an O_2-coordinating ability to the vesicles.

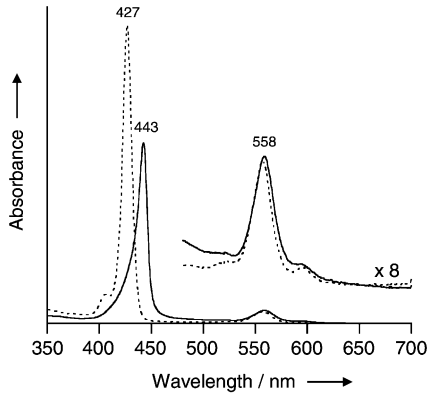

Figure 2. UV/Vis absorption spectra of **1b** at 25 °C: a) in benzene/MeOH (4:1 v/v) (dotted line) and b) in water (solid line).

Results and Discussion

Nanostructure and fluorescence of the lipid-porphyrin vesicles: The newly synthesized Zn^{2+} complex of lipid-porphyrin **1b** was dispersed in deionized water by ultrasonication to give a pink-colored colloidal solution. Transmission electron microscopy (TEM) of the negatively stained and evaporated sample on a copper grid showed that **1b** forms spherical unilamellar vesicles with a diameter of 100–150 nm as well as the corresponding free-base porphyrin **1a** and the Fe^{3+} complex **1c** (Figure 1a).[8c] The thickness of the membrane

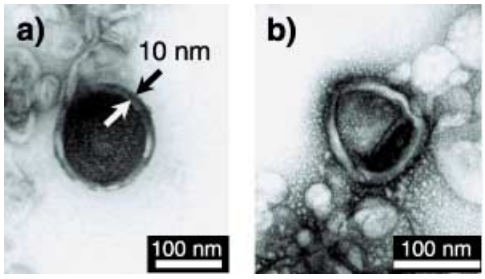

Figure 1. Transmission electron micrographs of evaporated aqueous solutions of a) **1b** and b) **1a**/**1b** ensemble (molar ratio: 1/1). The samples were negatively stained by uranylacetate.

was 10 nm, which is twice the molecular length of **1b** (4.6 nm). Most probably, the hydrophobic Zn^{2+}TPP platforms were arranged in two-dimensional planar sheets, which were stacked with a lateral displacement at the center of the membrane. It could be an identical conformation to that seen in the **1a** vesicles.[8c] The huge lipid-porphyrins (molecular weight over 4500) cannot produce a large curvature, so that they form giant unilamellar vesicles. This is in contrast to the fact that the usual phospholipids form small unilamellar vesicles (30–40 nm ϕ) by the same preparation.

The UV/Vis absorption spectrum of the aqueous solution of **1b** showed a porphyrin Soret band at 443 nm (ε_{max}: 2.7×10^5 $M^{-1}cm^{-1}$), and its maximum was red shifted (+16 nm) compared to that of the monomer in benzene/MeOH (4:1 v/v) solution (λ_{max}: 427 nm) (Figure 2). On the contrary, the porphyrin Q bands remained essentially unaltered (only a 1 nm red shift). This larger bathochromic shift of the Soret band should include excitonic interactions due to a lateral arrangement (J-aggregate) of the transition moments of the porphyrin chromophores.

We then did a quantitative analysis of the excitonic interactions of the bilayered Zn^{2+} porphyrin sheets according to our previously reported procedure.[8c] The simple point-dipole exciton coupling theory was employed,[9] and two hypotheses were postulated: 1) the tightest packing of the Zn^{2+}TPP moieties is realized within a rhomboidal lattice, which is observed in the triclinic unit cell of the single crystal of the unsolvated Zn^{2+}TPP (Figure 3, $2a$: 2.6 nm, $2b$: 1.48 nm),[10] and 2) the interlayer (d) of the face-to-face

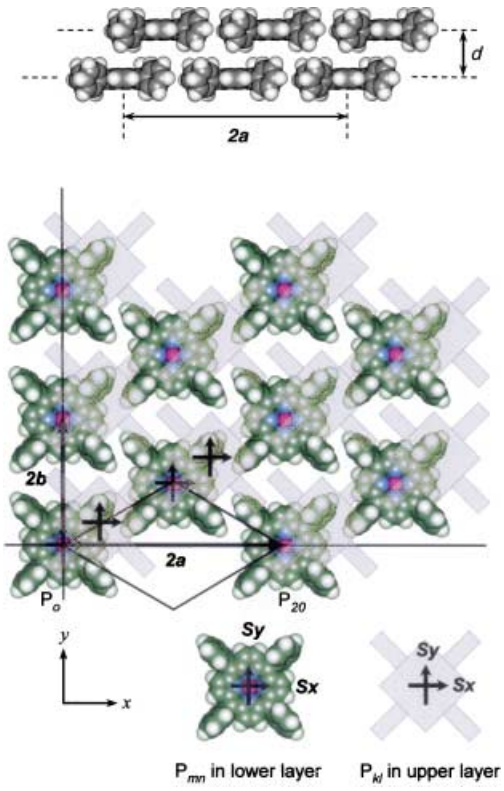

Figure 3. Predicted arrangements of the Zn^{2+}TPP platforms as a model for the bilayer membrane of **1b**. The porphyrin P_o is located at the origin of the coordinate axes.

stacking of the porphyrin sheets is 6.0 Å (Figure 3). The exciton interaction (ΔE) between the two porphyrins in the monolayer is given by Kasha's Equation (1).

$$\Delta E = M^2 r_{mn}^{-3} (1 - 3\cos^2\theta) \quad (1)$$

M is the transition dipole moment of the Zn^{2+}TPP moiety in **1b** ($M^2 = 68.2\,D^2$),[11] r_{mn} is the center-to-center distance between the original porphyrin o (P_o) and the porphyrin mn (P_{mn}), and θ is the tilt angle between the line of centers and the molecular axes. Using the same strategy, we can estimate the exciton interactions between P_o and the porphyrin kl in the upper layer (P_{kl}).[12] These calculations eventually gave the total differences V and V' in two different Soret transitions S_x and S_y as -612.3 and $-239.0\ cm^{-1}$, respectively, that indicate split Soret peaks of 430.8 and 437.5 nm. The observed Soret band was definitely asymmetric, and it could be divided into two absorptions (438.5 and 441.4 nm). The small difference between the calculated λ_{max} and experimentally measured values is likely to be due to the van der Waals shift caused by the replacement of solvents. Thus, we can conclude that the absorption shift in the Soret band is describable by exciton interaction. Of course, the observed shift in the Soret band comes from the averaged interaction and involves some deviations, because of the fluidity of the membranes.

The most remarkable photophysical property of the lipid-porphyrin vesicles is their strong fluorescence in comparison to the other porphyrin aggregates.[6, 8c] The 3D excitation-emission spectrum of the aqueous **1b** solution showed that the fluorescence emission maxima (λ_{em}: 601, 653 nm) correlated with the absorption of the vesicles (λ_{max}: 443 nm) (not shown), which suggests that the fluorescence comes from the membrane and not the monomer dissociated from the aggregate. Single photon-counting fluorescence measurements were also done in air-equilibrated solution of **1b** vesicle. The fluorescence decay profile could be analyzed in terms of a single exponential process with a lifetime (τ_F) of 1.35 ns ($\kappa^2 = 1.14$), which was slightly shorter than the value of the **1b** monomer in benzene/MeOH (4:1 v/v) solution ($\tau_F = 2.0$ ns). The excited triplet states of the **1b** vesicles are too short to be observed by our nanosecond laser flash photolysis apparatus.

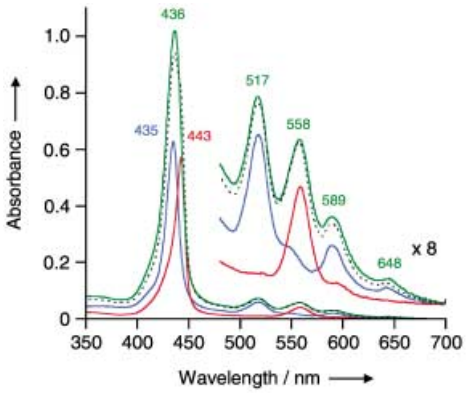

Figure 4. UV/Vis absorption spectra of **1a** vesicles (blue line), **1b** vesicles (red line), and **1a**/**1b** ensemble vesicles (molar ratio: 1/1, green line) in water at 25 °C. Black dotted lines represent the superposition of the spectra for **1a** and **1b**.

Energy transfer process within the lipid-porphyrin vesicles: Based on the exciton calculations, the alignment of the TPP planes in the free-base and the Zn^{2+} porphyrin vesicles would be identical. This result implies that they are able to produce homogeneous vesicular membranes. Indeed, the equivalent moles of **1a** and **1b** are spontaneously associated in water to yield spherical unilamellar vesicles with a diameter of 100–150 nm with a thickness of 10 nm (Figure 1b), in which the Zn^{2+} porphyrin should become the donor and the free-base porphyrin acts as the acceptor. The UV/Vis absorption spectrum of this **1a**/**1b** ensemble indicates that the spectral features are the sum of those from the individual lipid-porphyrin vesicles; it suggests no electronic interaction between **1a** and **1b** in the ground state (Figure 4). By contrast, its fluorescence spectrum is dramatically different from the superposition of those of the individual components. The **1a**/**1b** vesicles showed a decrease in fluorescence associated with the Zn^{2+} porphyrin and a corresponding increase in fluorescence associated with the free-base porphyrin (λ_{em}: 650, 712 nm) (Figure 5). Even on excitation at 558 nm, where the Zn^{2+} complex mainly absorbs (72%), the emission spectral shape obviously demonstrated that of the

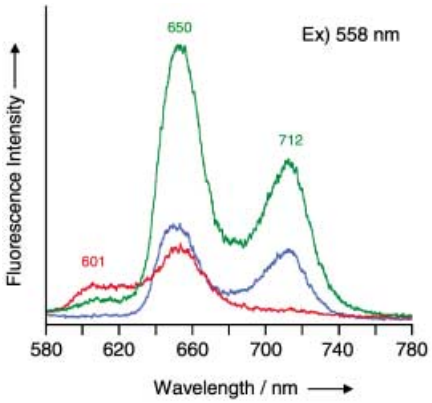

Figure 5. Steady-state fluorescence emission spectra of **1a** vesicles (blue line), **1b** vesicles (red line), and **1a**/**1b** ensemble vesicles (molar ratio: 1/1, green line) in water at 25 °C (Ex. 558 nm).

free-base porphyrin with stronger intensity by a factor of three. Because the fluorescence of the equivalent mixture of each vesicle solution displayed a simple sum of their spectra, efficient intermolecular singlet–singlet energy transfer could take place from the excited Zn^{2+} porphyrin donors to the statistically distributed free-base acceptor within the vesicles. Since the $\pi-\pi$ interactions between Zn porphyrins are usually somewhat stronger than those of the free-base porphyrins, there may not be a statistical dispersion of these two porphyrin chromospheres in the bilayer. However, for instance, the temperature dependence of the Soret band absorption maximum of the **1a**/**1b** vesicles showed a small hypsochromic shift at 56 °C, which suggests the gel-phase (liquid-crystal) transitions of the membrane. Very similar behavior was observed in the **1a** vesicles.[8a] This probably implied that the $\pi-\pi$ interactions between the Zn complexes are not so different from the free-bases in the lipid-porphyrin

vesicles. The fluorescence band of the donor considerably overlaps the acceptor absorption, therefore Förster-type excitation energy transfer would be preferable.[13]

The aqueous **1a**/**1b** vesicle solution was then transferred onto a graphite surface and subjected to near-field scanning optical microspectroscopy (NSOM). The bilayered membranes slowly flattened on the substrate during the water evaporation process. Unfortunately, the topology-mode measurements could not distinguish each 100 nm particle because of the low resolution. However, the dried vesicles still fluoresce on the solid surface and their emission was clearly detected by NSOM (Figure 6a). The fluorescence pattern of

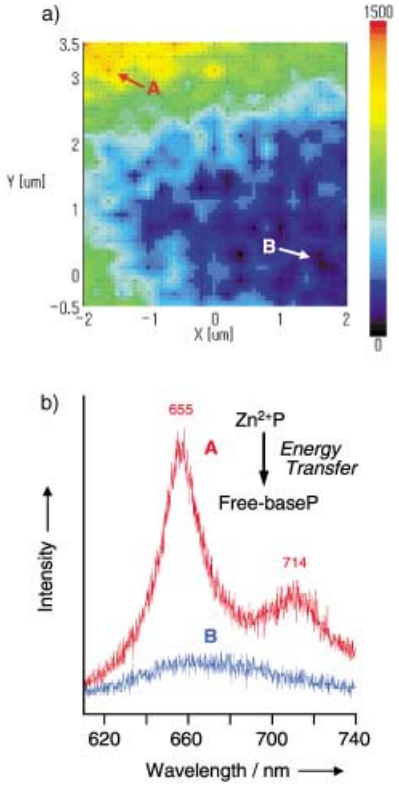

Figure 6. NSOM images of the evaporated aqueous solution of **1a**/**1b** ensemble vesicles (molar ratio: 1/1) on HOPG. a) fluorescence image of the flattened vesicles (4×4 μm, Ex. 442 nm, detection was effected at 650 nm), and b) fluorescence emission spectra of the flattened vesicles at the indicated parts [(A) and (B)] in the image a).

the collapsed **1a**/**1b** particles (λ_{em}: 655, 714 nm) was in good agreement with that of the free-base porphyrin [λ_{em}: 650, 712 nm, Figure 6b)]. Recently, Adams et al. reported interesting NSOM measurements of porphyrin thin films.[14] Our result is the first observation of an energy transfer molecular assembly made of amphiphilic porphyrin aggregates by the NSOM technique.

The fluorescence decay profile of this hybrid vesicle solution monitored at 610 nm became progressively triple-exponential with a faster decaying component being seen in addition to the original two slower kinetics ($\kappa^2 = 1.26$) (Figure 7). The longer lifetimes (6.73, 1.90 ns) are respectively assigned as those of **1a** and **1b**. The shorter-lived component (263 ps) is reflective of the singlet–singlet energy transfer

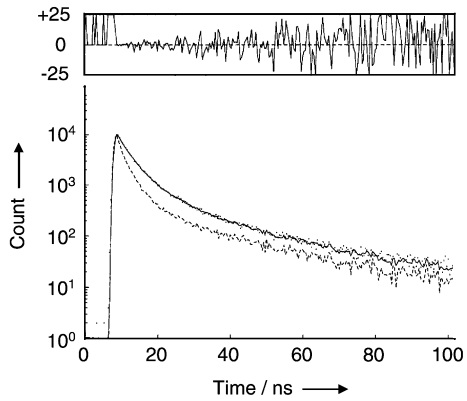

Figure 7. Time-correlated single-photon counting decay profile of **1a**/**1b** ensemble vesicles (molar ratio: 1/1, Ex. 558 nm, detection was effected at 610 nm). The curve is fitted to triple exponentials with lifetimes of 6.73 ns, 1.90 ns, and 263 ps ($\kappa^2 = 1.26$).

from the excited Zn^{2+} porphyrin to the free-base porphyrin within the vesicles. The rate constants for intermolecular energy transfer (k_{ET}) have been calculated from Equation (2).

$$k_{ET} = 1/\tau_{FB/Zn} - 1/\tau_{Zn} \quad (2)$$

$\tau_{FB/Zn}$ is the measured fastest component of the excited **1a**/**1b** vesicles and τ_{Zn} is the lifetime of the **1b** vesicles. The k_{ET} value was $3.1 \times 10^9\ s^{-1}$. The efficiency of this energy transfer (Φ_{ET}) could be determined to be 0.81 from Equation (3).[15]

$$\Phi_{ET} = k_{ET}/[k_{ET} + (1/\tau_{Zn})] \quad (3)$$

This non-covalently constructed **1a**/**1b** architecture showed relatively larger k_{ET} and Φ_{ET} than the values of the free-base/Zn^{2+} porphyrin dimers linked by covalent or hydrogen bonding.[2–5, 13] From the molecular area for lipid-porphyrin (2.2 nm^2), one vesicle (100 nm ϕ) is considered to consist of 23000 porphyrin molecules.[8c] To the best of our knowledge, this is the largest molecular energy transfer assembly made of self-organized porphyrin in water. For the triplet-state process, the transient difference absorption recorded in outgassed aqueous solution of the **1a**/**1b** vesicles did not show any significant peaks after the laser flash photolysis.

Electron transfer process of the lipid-porphyrin vesicles: In the lipid-porphyrin vesicles, the J-aggregated TPP platforms settled under the hydrophobic barrier of 4 nm thickness, and were not sensitive to the addition of a water-soluble electron acceptor or electron donor from the bulk aqueous phase. In fact, the fluorescence intensity of the **1a** or **1b** vesicles was not quenched at all by addition of electron acceptors; *N*,*N*′-methyl-4,4′-bipyridinium dichrolides and *N*,*N*′-benzyl-4,4′-bipyridinium dichrolides in the concentration range 0 to 2 mM. Since none of the quencher molecules caused a spectroscopic shift of the porphyrin absorption bands, there is no π-overlap between the electron accepting molecules and donating porphyrins. Attempting to reduce the Fe^{3+}TPP planes in the **1c** vesicles by addition of ascorbic acid also failed. These results imply that water-soluble molecules cannot enter the membrane interior. It is, therefore, certain

that the membrane properties should be modified to realize electron communications through the lipid-porphyrin membranes. Over the past few decades, substantial efforts have also been directed towards embedding two different porphyrins geometrically in phospholipid liposomes,[6f, 16] but the location of each co-factor is not always very accurate because of the low guest-to-host ratio in the membranes.

The free-base porphyrin **1a** was coassembled with protoporphyrin IX (PPIX) bearing two alkylphosphocholine propionates (**2**) (molar ratio: **1a**/**2** = 10), to give similar round vesicles. Although porphyrin **2** itself produced very thin monomolecular fibers in water (Figure 8a),[6d] the TEM observation showed only spherical unilamellars (ca. 100 nm

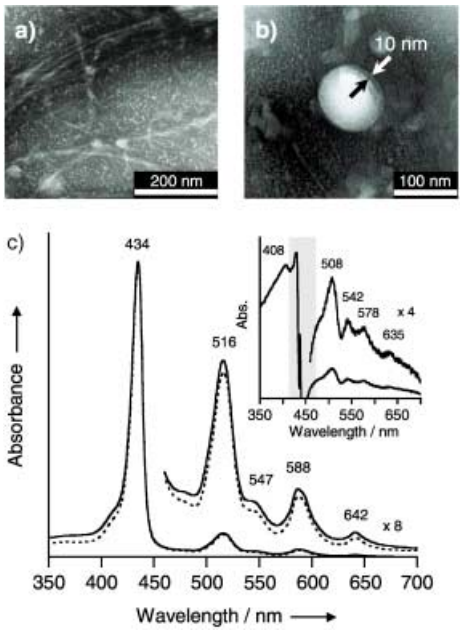

Figure 8. Transmission electron micrographs of the evaporated aqueous solutions of a) **2** and b) the **1a**/**2** ensemble (molar ratio: **1a**/**2** = 10); c) UV/Vis absorption spectra of **1a** vesicles (dotted line) and **1a**/**2** ensemble vesicles (solid line) in water at 25 °C. The inset shows a different spectrum for both solutions, in which the absorption maxima coincided with those of the DPPC vesicles incorporating **2** (molar ratio: DPPC/**2** = 40/1) in water.

ϕ) (Figure 8b). No fibrous aggregate was detectable and the membrane did not become thicker. Increasing the amount of **2** (molar ratio: **1a**/**2** < 5) led to deformation of the morphology into small micelles and fibers. The subtracted difference absorption spectrum of the **1a**/**2** hybrids minus the homogeneous **1a** vesicles showed λ_{max} at 408, 508, 542, 578, and 635 nm (Figure 8c inset). Unfortunately, the disturbance interfered with the Soret band region. It coincided with the absorption maxima of an aqueous solution of phospholipid liposomes (ex. 1,2-dipalmytoyl-3-*sn*-glycerophosphocholine (DPPC)) incorporating **2** (molar ratio: DPPC/**2** = 40, λ_{max}: 408, 509, 542, 579, and 634 nm). We concluded that **2** was homogeneously trapped into the highly oriented alkylene region of the **1a** vesicles without stacking. It may be presumed with certainty that the protoporphyrin macrocycle was anchored at the middle of the monolayer perpendicular to the membrane surface [see space-filling model in Figure 9b].

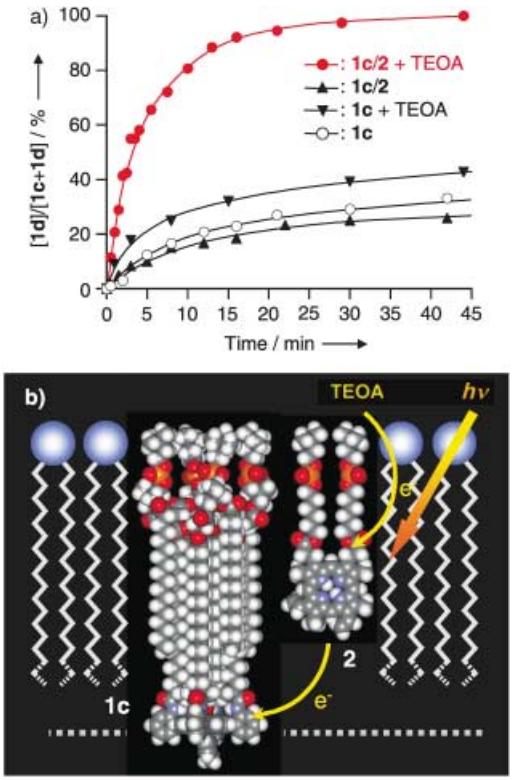

Figure 9. a) Photoreduction of Fe^{3+}TPP moieties of **1c**/**2**/DIm vesicles in aqueous phosphate buffer (pH 7.3) at 25 °C. b) The schematic representation of the **1c**/**2**/DIm monolayer membrane interior using the space-filling model for the each compound (DIm is replaced by 1-methylimidazole for clarification).

In the vesicles of the Fe^{3+} complex **1c** including free-base **2** (molar ratio: **1c**/**2** = 10), the fluorescence of the protoporphyrin chromophore was completely quenched. This decrease in the emission would be ascribed to the intermolecular electron transfer from the excited singlet state of **2** to **1c** within the vesicles. The Fe^{3+} porphyrins are *d*-typed hyperporphyrins with an extremely short lifetime of the excited state and no fluorescence. This quenching cannot be interpreted in terms of a static mechanism and is assumed to be due to oxidative quenching. An attempt to observe the time-resolved difference spectrum of the **2** cation radical was unsuccessful, because the absorption intensity of the protoporphyrin **2** was rather low, and the reaction rate was beyond the resolution of our apparatus. The excited triplet state of **2** may also be populated by means of intersystem crossing from the singlet state, which occurs in competition with the electron transfer, but the triplet – triplet absorption of **2** was not seen in the 500 – 900 nm region.

The coexistence of a small excess of 1-dodecylimidazole (DIm) as an axial base for the Fe^{3+} complex **1c** did not cause morphological changes in the vesicular configuration. The UV/Vis spectrum of the **1c**/**2**/DIm (molar ratio: 1/0.1/3) showed maxima at 544 and 575 nm, indicating that the dominant species of **1c** is a six-coordinate ferric complex with the axially bound bis-imidazole of DIm.[17] Under an argon atmosphere, the 390 nm (Soret band of **2**) photoirradiation of the **1c**/**2**/DIm vesicles with triethanolamine (TEOA) in the outer aqueous phase led to efficient and

irreversible reduction of the ferric ion of **1c**; the visible absorption spectrum changed to the typical six-*N*-coordinated low-spin Fe^{2+} complex (λ_{max}: 436, 538, and 568 nm).[8c, 18] The isosbestic points (534 and 562 nm) throughout the measurement revealed that no side reaction occurred. The following results indicate that the photoreduction of **1c** takes place through the intermolecular electron transfer initiated by excitation of **2**; 1) in the absence of TEOA or **2**, the reduction proceeded by less than 40% (Figure 9a), 2) irradiation of the Soret band of **1c** also reduced the ferric center, but by less than 30%. Photoirradiation of the Soret band of **2** causes only the efficient reduction of **1c**, and TEOA acts as a sacrificial reagent to reduce the cation radical of **2**. The protoporphyrin anchors successfully serve as an electron transfer mediator, and the space-filling model of the **1c**/**2**/DIm hybrid demonstrated well our supposed structure (Figure 9b). The overall process of this reaction is expressed by Equation (4), where LP is lipid-porphyrin and PP is the protoporphyrin moiety of **2**.

$$Fe^{3+}LP(DIm)_2 + PP \overset{h\nu}{\rightleftharpoons} Fe^{3+}LP(DIm)_2 + PP^* \rightleftarrows Fe^{2+}LP(DIm)_2 + PP^{+\cdot} \overset{e^-}{\rightleftharpoons} Fe^{2+}LP(DIm)_2 + PP \quad (4)$$

After reduction of **1c**, the membrane-trapped protoporphyrin becomes more hydrophilic and may be close enough to the bulk aqueous phase to accept an electron.

Upon exposure of the aqueous solution of the photoreduced **1d**/**2**/DIm vesicles to O_2, the UV/Vis absorption spectrum immediately changed to that of the corresponding O_2-adduct complex (λ_{max}: 435, 543 nm). This dioxygenation was observed to be reversibly dependent on the O_2-partial pressure the same as in our previous reported **1d**/DIm vesicles.[8c]

Conclusions

The perfectly round bilayer vesicles made of self-organized lipid-porphyrin **1a**/**1b** ensembles are the first molecular energy transfer assemblies with a diameter of over 100 nm in water. Singlet energy transfer occurs with a rate constant of $3.1 \times 10^9\ s^{-1}$ and with 81% efficiency. The non-covalently aligned J-aggregate porphyrins described herein have been shown to represent an effective approach to constructing a new class of light-harvesting antennae models in aqueous media. Indeed, effective optical cross-section per **1b** molecule in the vesicles at 558 nm is 0.73 Å^2, which is identical to that observed in benzene/MeOH homogeneous solution.[19] The 23000 porphyrin active sites are densely packed in the vesicles and isolated from the bulk aqueous solution; therefore electron communications to the outside of the membrane have some difficulties. However, anchoring of the protoporphyrin electron-mediator to the monolayer immediately permits funneling an electron by light irradiation, and it gave a hemoglobin-like property—reversible O_2-binding activity—to the vesicles. New investigations of a photoinduced charge separation process with an external electron acceptor and light-controllable heme catalytic reactions in these supramolecular lipid-porphyrin architectures are now being undertaken.

Experimental Section

Materials and apparatus: The synthetic methods for lipid-porphyrins (**1a**, **1c**, **2**) are described elsewhere.[8c, 6d] The Zn^{2+} complex **1b** was synthesized by the insertion of zinc into the free-base lipid-porphyrin **1a** using $Zn(OAc)_2$ in MeOH solution (yield: 85%). Triethanolamine, *N*,*N*′-methyl-4,4′-bipyridinium dichrolides, and *N*,*N*′-benzyl-4,4′-bipyridinium dichrolides of high-purity grade were used without further purification. UV/Vis absorption spectra were recorded on a JASCO V-570 spectrophotometer, and steady state fluorescence spectra were obtained from a HITACHI F-4500 spectrofluorometer. All these measurements were normally carried out at 25 °C.

Preparation of aqueous lipid-porphyrin solutions:

*a) Lipid-porphyrin (**1a**, **1b**, **1a**/**1b**) solutions*: A benzene/methanol stock solution of **1a** or **1b** (50—100 μL, 1.0 mM) was placed in a 5 mL round-bottom flask and slowly condensed using a rotary evaporator under reduced pressure, affording a thin film of the porphyrin at the bottom. The film was then dried in vacuo for 3 h; deionized water (5 mL) heated at 60 °C was slowly injected. The mixture was homogenized by vortex mixing with several small glass beads (ca. 10 pieces) and shortly sonicated by a bath-type ultrasonicator. The obtained solution (10–20 μM) was incubated for 6 h at room temperature before use. The hybridized **1a**/**1b** solution was also prepared in the same manner.

*b) Lipid-porphyrins **1a**/**2** and **1c**/**2**/1-dodecylimidazole (DIm) hybrid solutions*: A benzene/methanol stock solution of **1a** (100 μL, 1.0 mM) and methanol solution of **2** (10 μL, 1.0 mM) were slowly condensed by using a rotary evaporator under reduced pressure as described above, giving a hybrid thin-film at the bottom of the flask. The film was dried *in vacuo* for 3 h and phosphate buffer (pH 7.3, 1 mM, 5 mL) heated at 60 °C was added. Homogenization by a tip-type ultrasonicator (60 mW, 3 min) in a water bath provided a pale orange solution ([**1a**] = 20 μM), which was incubated for 12 h at room temperature. The hybrid lipid-porphyrin **1c**/**2**/DIm (molar ratio: 1/0.1/3, [**1c**] = 20 μM) was also prepared by the same procedures.

Transmission electron microscopy (TEM): The negatively stained specimens for TEM were prepared as in previously reported procedures.[7c, 8b] The Cu grid surfaces were treated for a short period (5 s) by glow discharge using a JEOL HDF-400 to form a hydrophilic plane just before use. The obtained grids with the evaporated sample were observed in a JEOL JEM-100CX electron microscope at an acceleration voltage of 100 kV.

Exciton calculation: The overall excitonic interaction in the Zn^{2+}TPP bilayer model of **1b** was calculated based on our previously reported methods.[8c]

Near-field scanning optical microspectroscopy (NSOM): A droplet of **1a**/**1b** vesicle solution (20 μM) was pipetted onto freshly-cleaved highly-oriented pyrolytic graphite (HOPG STM-1, Advanced Ceramics Co.). After 1 min, excess fluid was carefully blotted off with filtration paper and the surface air-dried for another 30 min. NSOM measurements were carried out using a JASCO NFS-230 Scanning Near-Field Optical Microspectrometer in the illumination collection mode under ambient laboratory conditions. The samples were excited by a He-Cd laser (442 nm) with 0.1 mW intensity for 0.5 s, and the diameter of the light probe was 400 nm. Imaging was performed by displaying the fluorescence signal and the height signal simultaneously for 4×4 μm (21×21 points).

Excited-state lifetimes: Singlet lifetimes of the lipid-porphyrin vesicles were measured by using a HORIBA NAES-500 nanosecond fluorometer with an N_2 lamp (excitation side multicavity filter: ASAHI SPECTRA MZ0560, $\lambda = 560 \pm 2$ nm; emission side multicavity filter: MZ0610, $\lambda = 610 \pm 2$ nm). The samples were held in a cuvette (optical path length, 10 mm). The concentration of the lipid-porphyrin was 9.5 μM, and experiments were carried out at 25 °C. Triplet lifetime measurements on a nanosecond time scale were performed by using a Unisoku TSP-600 time-resolved spectrophotometer system with a Continuum Surelite I-10 Q-switched Nd-YAG laser, which generated a second-harmonic (532 nm) pulse of 6 ns duration with an energy of 200 mJ per pulse (10 Hz).

Steady-state electron-transfer from excited 2 to 1c: Continuous light irradiations were performed with an ORIEL 450 W xenon arc-lamp model 66021 under an argon atmosphere (25 °C). The **1c** solution was deaerated by argon bubbling before photoirradiation. The light was filtered with cutoff filter (HOYA UV-32) and a multicavity filter (ASAHI SPECTRA

MY0390, $\lambda = 390 \pm 2$ nm) to isolate the desired wavelength region. The filtered light was irradiated into a solution of the **1c**/DIm (molar ratio: 1/3) vesicles or **1c**/**2**/DIm vesicles (molar ratio: **1c**/**2**/DIm = 1/0.1/3) with (or without) triethanolamine (64 mM) contained in a 10 mm cuvette at a distance of 140 mm from the center of the light source. The UV/Vis absorption spectra of the solution were measured at regular intervals. The photoreduction of **1c** to the ferrous complex **1d** was monitored by the time dependence of the absorption intensity at 538 nm, which is based on the bisimidazole coordinated Fe^{2+} complex. In order to obtain a spectrum of the completely reduced ferrous **1d**/**2**/DIm vesicles, an aqueous sodium dithionate solution (25 mM, 40 μL) was added to the **1c**/**2**/DIm vesicle solution at 60 °C.

Acknowledgements

We thank the JASCO Corporation for the skilful observations of NSOM. This work was partially supported by a Grant-in-Aid for Scientific Research (No. 13650938) from the JSPS, and Health Science Research Grants (Research on Pharmaceutical and Medical Safety) from the MHLW.

[1] a) J. Deisenhofer, O. Epp, K. Miki, R. Huber, H. Michel, *Nature* **1985**, *318*, 618–624; b) G. Feher, J. P. Allen, M. Y. Okamura, D. C. Rees, *Nature* **1989**, *339*, 111–116; c) G. McDermott, S. M. Prince, A. A. Freer, A. M. Hawthornthwaite-Lawless, M. Z. Papiz, R. J. Cogdell, N. W. Isaacs, *Nature* **1995**, *374*, 517–521; d) S. M. Prince, M. Z. Papiz, A. A. Freer, G. McDemott, A. M. Hawthornthwaite-Lawless, R. J. Codgell, N. W. Isaacs, *J. Mol. Biol.* **1997**, *268*, 412–423; e) J. M. Olson, *Photochem. Photobiol.* **1998**, *67*, 61–75.

[2] a) M. R. Wasielewski, *Chem. Rev.* **1992**, *92*, 435–461; b) J. K. M. Sanders in *The Porphyrin Handbook, Vol. 3, Inorganic, Organometallic and Coordination Chemistry* (Eds.: K. M. Kadish, K. M. Smith, R. Guilard), Academic Press, New York, **1999**, Chapter 22.

[3] Examples of covalently bound multiporphyrinic assemblies made of more than three porphyrin units: a) S. Anderson, H. L. Anderson, A. Bashall, M. McPartlin, J. K. M. Sanders, *Angew. Chem.* **1995**, *107*, 1196–1200;*Angew. Chem. Int. Ed. Engl.* **1995**, *34*, 1096–1099; b) C. C. Mak, N. Bampos, J. K. M. Sanders, *Angew. Chem.* **1998**, *110*, 3169–3172; *Angew. Chem. Int. Ed.* **1998**, *37*, 3020–3023; c) H. A. M. Biemans, A. E. Rowan, A. Verhoeven, P. Vanoppen, L. Latterini, J. Foekema, A. P. H. J. Schenning, E. W. Meijer, F. C. de Schryver, R. J. M. Nolte, *J. Am. Chem. Soc.* **1998**, *120*, 11054–11060; d) M. G. H. Vicente, M. T. Cancilla, C. B. Lebrilla, K. M. Smith, *Chem. Commun.* **1998**, 2355–2356; e) A. Nakano, A. Osuka, I. Yamazaki, T. Yamazaki, Y. Nishimura, *Angew. Chem.* **1998**, *110*, 3172–3176; *Angew. Chem. Int. Ed.* **1998**, *37*, 3023–3027; f) N. Aratani, A. Osuka, Y.-H. Kim, D.-H. Jeong, D. Kim, *Angew. Chem.* **2000**, *112*, 1517–1521; *Angew. Chem. Int. Ed.* **2000**, *39*, 1458–1462; g) J. Li, A. Ambroise, S.-I. Yang, J. R. Diers, J. Seth, C. R. Wack, D. F. Bocian, D. Holten, J. S. Lindsey, *J. Am. Chem. Soc.* **1999**, *121*, 8927–8940; h) M.-S. Choi, T. Aida, T. Yamazaki, I. Yamazaki, *Angew. Chem.* **2001**, *113*, 3294–3298; *Angew. Chem. Int. Ed.* **2001**, *40*, 3194–3198; i) S. Rucareanu, O. Mongin, A. Schuwey, N. Hoyler, A. Gossauer, *J. Org. Chem.* **2001**, *66*, 4973–4988.

[4] J. L. Sessler, B. Wang, S. L. Spring, C. T. Brown in *Comprehensive Supramolecular Chemistry, Supramolecular Reactivity and Transport: Bioorganic Systems, Vol. 4* (Eds.: J.-M. Lehn, J. L. Atwood, J. E. D. Davies, D. D. MacNicol, F. Vögtle, Pergamon), Oxford, **1996**, pp. 311–336.

[5] Examples of noncovalently bound multiporphyrinic assemblies made of more than three porphyrin units: a) A. M. Brun, S. J. Atherton, A. Harriman, V. Heitz, J.-P. Sauvage, *J. Am. Chem. Soc.* **1992**, *114*, 4632–4639; b) M. Linke, J.-C. Chambron, V. Heitz, J.-P. Sauvage, S. Encinas, F. Barigelletti, L. Flamigni, *J. Am. Chem. Soc.* **2000**, *122*, 11834–11844; c) J. L. Sessler, B. Wang, A. Harriman, *J. Am. Chem. Soc.* **1995**, *117*, 704–714; d) H. L. Anderson, *Inorg. Chem.* **1994**, *33*, 972–981; e) G. S. Wilson, H. L. Anderson, *Chem. Commun.* **1999**, 1539–1540; f) C. A. Hunter, R. K. Hyde, *Angew. Chem.* **1996**, *108*, 2064–2067; *Angew. Chem. Int. Ed. Engl.* **1996**, *35*, 1936–1939; g) R. A. Haycock, A. Yartsev, U. Michelson, V. Sundström, C. A. Hunter, *Angew. Chem.* **2000**, *112*, 3762–3765; *Angew. Chem. Int. Ed.* **2000**, *39*, 3616–3619; h) P. Ballester, R. M. Gomila, C. A. Hunter, A. S. H. King, L. J. Twyman, *Chem. Commun.* **2003**, 38–39; i) C. M. Drain, K. C. Russel, J.-M. Lehn, *Chem. Commun.* **1996**, 337–338; j) J. Fan, A. Whiteford, B. Olenyuki, M. D. Levin, P. J. Stang, E. B. Fleischer, *J. Am. Chem. Soc.* **1999**, *121*, 2741–2752; k) A. Prodi, M. T. Indelli, C. J. Kleverlaan, F. Scandola, E. Alessio, T. Gianferrara, L. G. Marzilli, *Chem. Eur. J.* **1999**, *5*, 2668–2679; l) N. Maruo, M. Uchiyama, T. Kato, T. Arai, H. Akisada, N. Nishino, *Chem. Commun.* **1999**, 2057–2058; m) K. Ogawa, Y. Kobuke, *Angew. Chem.* **2000**, *112*, 4236–4239; *Angew. Chem. Int. Ed.* **2000**, *39*, 4070—4073; n) C. C. Mak, N. Bampos, S. L. Darling, M. Montalti, L. Prodi, J. K. M. Sanders, *J. Org. Chem.* **2001**, *66*, 4476–4486; o) M. Sakamoto, A. Ueno, H. Mihara, *Chem. Eur. J.* **2001**, *7*, 2449–2458; p) S. Yagai, T. Miyatake, H. Tamiaki, *J. Org. Chem.* **2002**, *67*, 49–58.

[6] R. Guilard, N. Senglet, Y. H. Liu, D. Sazou, E. Findsen, D. Fanre, T. D. Courieres, K. M. Kadish, *Inorg. Chem.* **1991**, *30*, 1898–1905; b) J.-H. Fuhrhop, C. Demoulin, C. Böttcher, J. Köning, U. Siggel, *J. Am. Chem. Soc.* **1992**, *114*, 4159–4165; c) J.-H. Fuhrhop, U. Bindig, U. Siggel, *J. Am. Chem. Soc.* **1993**, *115*, 11036–11037; d) E. Tsuchida, T. Komatsu, N. Toyano, S. Kumamoto, H. Nishide, *J. Chem. Soc. Chem. Commun.* **1993**, 1731–1733; e) T. Komatsu, K. Arai, H. Nishide, E. Tsuchida, *Chem. Lett.* **1993**, 1949–1952; f) T. Komatsu, E. Tsuchida, C. Böttcher, D. Donner, C. Messerschmidt, U. Siggel, W. Stocker, J. P. Rabe, J.-H. Fuhrhop, *J. Am. Chem. Soc.* **1997**, *119*, 11660–11665; g) C. Schell, H. K. Hombrecher, *Chem. Eur. J.* **1999**, *5*, 587–598; h) K. Kano, K. Fukuda, H. Wakami, R. Nishiyabu, R. F. Pasternack, *J. Am. Chem. Soc.* **2000**, *122*, 7494–7502; i) N. Nagata, S. Kugimiya, Y. Kobuke, *Chem. Commun.* **2001**, 689–690.

[7] a) T. Komatsu, K. Nakao, H. Nishide, E. Tsuchida, *J. Chem. Soc., Chem. Commun*. **1993**, 728–730; b) E. Tsuchida, T. Komatsu, K. Arai, K. Yamada, H. Nishide, C. Böttcher, J.-H. Fuhrhop, *Chem. Commun.* **1995**, 1063–1064; c) T. Komatsu, K. Yamada, E. Tsuchida, U. Siggel, C. Böttcher, J.-H. Fuhrhop, *Langmuir* **1996**, *12*, 6242–6249; d) T. Komatsu, T. Yanagimoto, E. Tsuchida, U. Siggel, J.-H. Fuhrhop, *J. Phys. Chem. B* **1998**, *102*, 6759–6765; e) T. Komatsu, T. Yanagimoto, Y. Furubayashi, J. Wu, E. Tsuchida, *Langmuir* **1999**, *15*, 4427–4433.

[8] a) E. Tsuchida, T. Komatsu, K. Arai, H. Nishide, *J. Chem. Soc., Chem. Commun.* **1993**, 730–732; b) E. Tsuchida, T. Komatsu, K. Arai, K. Yamada, H. Nishide, C. Böttcher, J.-H. Fuhrhop, *Langmuir* **1995**, *11*, 1877–1884; c) T. Komatsu, M. Moritake, A. Nakagawa, E. Tsuchida, *Chem. Eur. J.* **2002**, *8*, 5469–5480.

[9] a) E. G. McRae, M. Kasha, *J. Chem. Phys.* **1958**, *28*, 721–722; b) M. Kasha, *Radiation Res.* **1963**, *20*, 51–71.

[10] a) M. P. Byrn, C. J. Curtis, I. Goldberg, Y. Hsiou, S. I. Khan, P. A. Sawin, S. K. Tendick, C. E. Strouse, *J. Am. Chem. Soc.* **1991**, *113*, 6549–6557; b) M. P. Byrn, C. J. Curtis, Y. Hsiou, S. I. Khan, P. A. Sawin, S. K. Tendick, A. Terzis, C. E. Strouse, *J. Am. Chem. Soc.* **1993**, *115*, 9480–9497.

[11] The transition dipole moment was calculated by integrating plots of exciton coefficient divided by wavenumber, $\varepsilon(\nu)/\nu$, versus wavenumber ν and applying the equation $M^2 = 9.19 \times 10^{-3} \int[\varepsilon(\nu)/\nu]\mathrm{d}\nu$, where M is the transition dipole moment in units of Debye.

[12] Based on the structural data reported by Strauce et al. (ref. [10]), the porphyrin core in the upper layer is supposed to locate on the +4.0, +2.7, and +4.1 Å shifts in the x, y, z directions from the center of each nearest pair in the layer below. The distances and angles from the porphyrin o to the neighbors P_{kl} in the upper layer were estimated. We then calculated all the interactions of these porphyrin pairs (total: 46 combinations), but stopped summation at a distance of some 5 nm.

[13] a) F. P. Schwarz, M. Gouterman, Z. Muljiani, D. H. Dolphin, *Bioinorg. Chem.* **1972**, *2*, 1–32; b) R. L. Brookfield, H. Ellul, A. Harriman, G. Porter, *J. Chem. Soc. Faraday Trans. 2* **1986**, *82*, 219–233; c) A. Osuka, K. Maruyama, I. Yamazaki, N. Tamai, *Chem. Phys. Lett.* **1990**, *165*, 392–396.

[14] D. M. Adams, J. Kerimo, C.-Y. Liu, A. J. Bard, P. F. Barbara, *J. Phys. Chem. B* **2000**, *104*, 6728–6736.

[15] Apparent energy transfer efficiency estimated from the steady state fluorescence intensity at 610 nm (Figure 5) was 0.61 (ref. [13b]).

[16] a) J. Lahiri, G. D. Fate, S. B. Ungashe, J. T. Groves, *J. Am. Chem. Soc.* **1996**, *118*, 2347–2358; b) C. R. Drain, *Proc. Natl. Acad. Sci. USA*, **2002**, 99, 5178–5182.
[17] a) F. A. Walker, M.-W. Lo, M. T. Ree, *J. Am. Chem. Soc.* **1976**, *98*, 5552–5560; b) R. Quinn, M. Nappa, J. S. Valentine, *J. Am. Chem. Soc.* **1982**, *104*, 2588–2595.
[18] a) J. P. Collman, R. R. Gagne, C. A. Reed, T. R. Halbert, G. Lang, W. T. Robinson, *J. Am. Chem. Soc.* **1975**, *97*, 1427–1439; b) J. R. Budge, P. E. Ellis, Jr., R. D. Jones, J. E. Linard, F. Basolo, J. E. Baldwin, R. L. Dyer, *J. Am. Chem. Soc.* **1979**, *101*, 4760–4762; c) M. Momenteau, B. Loock, E. Bisagni, M. Rougee, *Can. J. Chem.* **1979**, *57*, 1804–1813.
[19] a) D. Mauzerall, N. L. Greenbaum, *Biochim. Biophys. Acta* **1989**, *974*, 119–140; b) N. L. Greenbaum, D. Mauzerall, *Biochim. Biophys. Acta* **1991**, *1057*, 195–207.

Received: April 3, 2003 [F5013]

